

Joule heating in ferromagnetic nanowires: Prediction and observation

Kab-Jin Kim,¹ Jae-Chul Lee,¹ Sug-Bong Choe,^{1,a)} and Kyung-Ho Shin²

¹School of Physics, Seoul National University, Seoul 151-742, Republic of Korea

²Nano-Device Research Center, Korea Institute of Science and Technology, Seoul 136-791, Republic of Korea

(Received 23 January 2008; accepted 15 April 2008; published online 15 May 2008)

We present an analytic theory of the Joule heating in metallic nanowires. The steady state is calculated for heat conduction through the insulation layer and then the transient state is considered from the thermodynamics law. The temperature is predicted to exhibit a quick exponential decay to a steady state within a few tens of nanoseconds. The decay time is linearly dependent on the temperature coefficient and both increase to saturation values with the increasing wire width. The validity of the theory is experimentally confirmed by the *in situ* measurement of the temperature-dependent electric resistance. © 2008 American Institute of Physics.

[DOI: 10.1063/1.2926374]

The current-induced magnetization dynamics provides great opportunities in magnetism.^{1,2} Various phenomena have been demonstrated for challenging the technological applications.³⁻⁷ To generate such effects, however, considerable current is required, which is essentially accompanied with the Joule heating.^{8,9} Yamaguchi *et al.*¹⁰ reported that the temperature even exceeded the Curie temperature. You *et al.*¹¹ proposed a theory for nanowires on infinitely thick insulator, which predicts an infinite temperature rising. The same authors derived the finite temperature rising for the finite insulator thickness with some adjusting parameters.¹² In this letter, we present a rigorous analytic expression of the steady-state temperature under the Joule heating followed by the extension of the theory to the transient state for the pulsed current. The validity of the theory is confirmed by the *in situ* measurements of the temperature-dependent electric resistance.

The nanowire sample generally has a structure depicted in Fig. 1(a). Here, the nanowire with the thickness h and the width w is placed on the electric insulation layer with the thickness d on the top of the substrate. The insulation layer has a much smaller thermal conductivity compared to the substrate and thus, it is natural to expect that the temperature variation inside the substrate is negligible. We assume a constant substrate temperature T_0 . The situation then becomes equivalent to the case of mirrored images, as illustrated in Fig. 1(b). In the mirrored structure, the nanowire generates the heat s_0 , whereas the mirrored nanowire absorbs the heat. The Joule heating rate per unit area is given by $s_0 = \rho h J^2$ for the current density J with the resistivity ρ .

Due to the wire geometry, we solve the two-dimensional heat conduction equation through the insulation layer. The steady-state solution is given by $T(x, z) - T_0 = K_I^{-1} \int_{C'} G(x, z; x', z') s(x', z') dC'$ for the surface C' , where K_I is the thermal conductivity of the insulation layer, and s is the surface heat source and sink. Using the Green function $G(x, z; x', z') = (4\pi)^{-1} \log[(x-x')^2 + (z-z')^2]$, one can carry out the integration and obtain the solution as

$$T(x, z) - T_0 = \frac{\rho h J^2}{4\pi K_I} \left[f\left(\frac{w}{2} + x, d + z\right) + f\left(\frac{w}{2} - x, d + z\right) - f\left(\frac{w}{2} + x, d - z\right) - f\left(\frac{w}{2} - x, d - z\right) \right], \quad (1)$$

where $f(a, b) = 2b \tan^{-1}(a/b) + a \log(a^2 + b^2)$. Finally, the average temperature T_W^{eq} over the nanowire is given by

$$\Delta T_W^{\text{eq}} = T_W^{\text{eq}} - T_0 = \frac{1}{w} \int_{-w/2}^{w/2} T(x, d) dx = \frac{\rho h d J^2}{K_I} \xi\left(\frac{w}{2d}\right), \quad (2)$$

where $\xi(\alpha) = 2\pi^{-1} [\tan^{-1} \alpha + (1/4)\alpha \log(1 + \alpha^2) - (1/4)\alpha^{-1} \log(1 + \alpha^2)]$. The present result is consistent with the previous theories for limiting cases, i.e., $\Delta T_W^{\text{eq}} \sim \rho w h J^2 \log d / 2\pi K_I$ for $d \gg w$ ¹¹ and $\Delta T_W^{\text{eq}} \sim \rho h d J^2 / K_I$ for $d \ll w$.¹²

To extend the theory to the transient state, we adopt the thermodynamic consideration for quasistatic process. The internal thermal energy stored in the nanowire of the length l is given by $U_W^{\text{eq}} = c_W w h l (T_W^{\text{eq}} - T_0)$. Similarly, the internal energy in the insulation layer is $U_I^{\text{eq}} = c_I l \int_0^d \int_{-\infty}^{\infty} T(x, z) dx dz = c_I w d l (T_W^{\text{eq}} - T_0) / 2\xi$. Here, c_W and c_I are the heat capacity per unit volume of the nanowire and insulator materials, respectively. The quasistatic change in the total internal energy is then $dU = dT_W (2c_W w h l \xi + c_I w d l) / 2\xi$, which is subjected to $dU = dQ_{\text{Joule}} - dQ_{\text{conduction}}$ based on the law of thermodynamics. Here, the Joule heating is given by $dQ_{\text{Joule}} = \rho w h l J^2 dt$ and the heat conduction to the substrate through the insulation layer is $dQ_{\text{conduction}} = (K_I w' l / d) (T_W - T_0) dt$, where w' is the effective width for heat conduction. Comparing with the steady-state

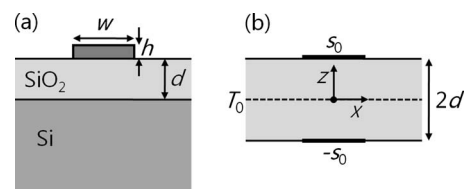


FIG. 1. (a) Cross-sectional view of the sample structure. (b) Equivalent geometry with mirrored images within the assumption of a constant substrate temperature T_0 .

^{a)}Electronic mail: sugbong@snu.ac.kr.

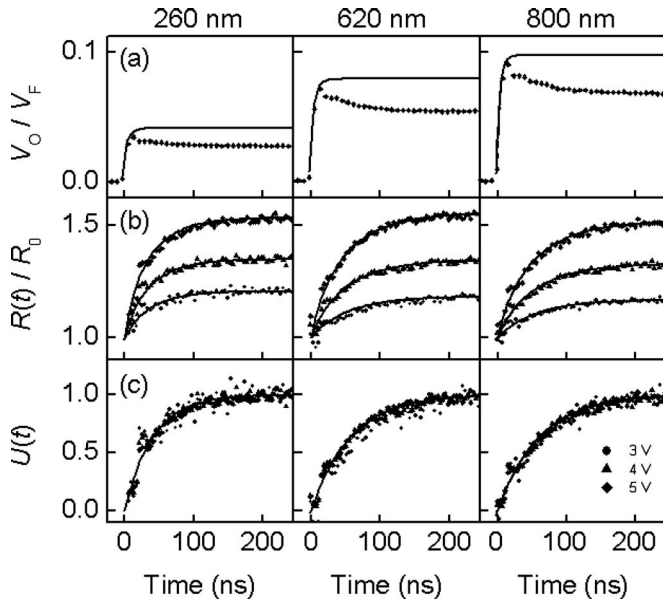


FIG. 2. (a) The outgoing voltage profile in time for $V_F=5$ V (diamond symbol) and $V_F\leq 1$ V (solid line). (b) The resistance variation in time for several pulse voltage as denoted in the figure. (c) The universal function for several pulse voltages. The solid lines are the best fit from Eq. (5).

solution, the effective width w' must equal to w/ξ . Solving the final differential equation, one can obtain the exponential decay to the steady state as given by

$$T_w(t) - T_0 = \Delta T_w^{eq} [1 - \exp(-t/\tau)], \quad (3)$$

with the decay time $\tau = (2c_w h d \xi (w/2d) + c_l d^2) / 2K_l$.

For more realistic experimental situation, we incorporate the temperature dependence of the resistance. It is empirically given by $\rho = \rho_0 [1 + \alpha(T - T_0)]$ or $R = R_0 [1 + \alpha(T - T_0)]$, with the temperature coefficient α . Replacing ρ in Eq. (2), we obtain

$$\Delta T_w^{eq} = \frac{\beta J^2}{\alpha(1 - \beta J^2)} \text{ or } R^{eq} = \frac{R_0}{1 - \beta J^2}, \quad (4)$$

with the coefficient $\beta = \alpha \rho_0 h d \xi (w/2d) / K_l$. For constant voltage pulse injection, the Joule heating term is modified to $dQ_{Joule} = whl(V/l)^2 dt / \rho_0 (1 + \alpha(T_w - T_0))$ and the transient state solution is given by introducing a universal function as

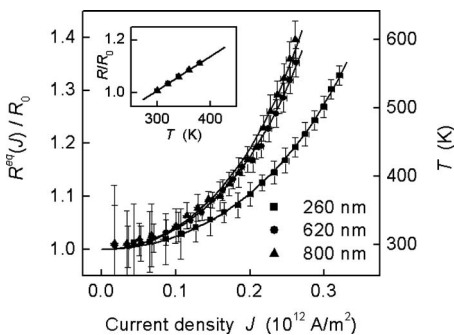


FIG. 3. The saturation temperature with respect to the current density. The solid lines are the best fit curves from Eq. (4). (inset) The temperature dependence of the resistance measured in a cryostat.

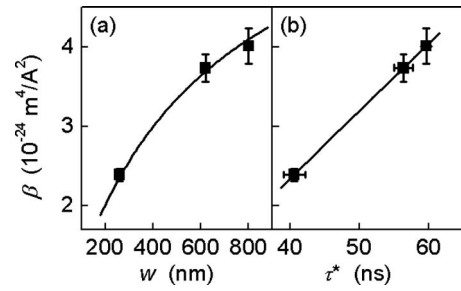


FIG. 4. (a) The temperature parameter β with respect to the wire width. The solid line exhibits the theoretical prediction. (b) The linear dependence between the temperature parameter β and the decay time τ^* .

$$U(t) \equiv \left(\frac{R(t)}{R^{eq}} \right) \left(\frac{R(t) - R_0}{R^{eq} - R_0} \right) \cong 1 - \exp(-t/\tau^*), \quad (5)$$

for a small voltage. The decay time here is given by $\tau^* = \tau/2 = c_w \beta / 2\alpha \rho_0 + c_l d^2 / 4K_l$.

The validity of the theory is confirmed by the experimental measurements. The experimental procedure is as follows. We inject a voltage pulse V_F into one end of the Permalloy nanowire and monitor the outgoing voltage pulse V_O from the other end.¹³ The resistance R of the nanowire is then calculated by the circuit equation $R = R_O(V_F/V_O - 1) - R_F$, where R_O and R_F are the load resistance of the oscilloscope and the function generator, respectively. Finally, the temperature of the nanowire is estimated from the experimentally determined α for each nanowire.

Figure 2(a) shows the observed oscilloscope voltage V_O normalized by V_F . The diamond symbols show the outgoing voltage profile for $V_F=5$ V. For comparison, the voltage profile for $V_F\leq 1$ V is shown by the solid line. It is clear from the figure that the outgoing voltage quickly drops down within a few tens of nanoseconds for a high pulse voltage. The voltage drop is ascribed to the resistivity increment caused by the Joule heating. Based on the outgoing voltage profile, the resistance variation in time is calculated, as plotted in Fig. 2(b) for several pulse voltages.¹⁴ As predicted, all the curves in Fig. 2(b) gather into a universal curve, as seen in Fig. 2(c). The solid lines show the best fit using Eq. (5).

The steady-state temperature is plotted with respect to the current density in Fig. 3. The inset shows the measurement of the temperature coefficient α . The temperature is perfectly matched to the solid line of the best fit from Eq. (4). Figure 4(a) shows the fitting value β with respect to the wire width. The values quantitatively fit to the solid line from the theoretical prediction. The theoretical prediction is obtained by using the values of the wire geometry $h=29$ nm and $d=300$ nm, the experimentally determined material parameters $\alpha = (1.29 \pm 0.01) \times 10^{-3} \text{ K}^{-1}$ and $\rho_0 = (7.5 \pm 0.3) \times 10^{-7} \text{ } \Omega \text{ m}$, and the thermal conductivity $K_{\text{SiO}_2} = 1.16 \text{ W/m K}$. The linear dependence between β and τ^* is also experimentally confirmed in Fig. 4(b). The experimental $d\beta/d\tau^*$ is found to be a little bit larger than the bulk-value-based prediction. It is possibly ascribed to the interface imperfection and/or interface diffusion barrier formation, which impedes the thermal diffusion.

This study was supported by the Korea Science and Engineering Foundation (2005-02172, R0A-2007-000-20032-0). K.J.K. was supported by the Korea Research Foundation (KRF-2005-205-C00010). K.H.S. was supported

by the KIST Institutional program, by the TND Frontier Project funded by KISTEP, and by the Korea Research Council of Fundamental Science & Technology (KRCF).

¹J. C. Slonczewski, *J. Magn. Magn. Mater.* **159**, L1 (1996).

²L. Berger, *Phys. Rev. B* **54**, 9353 (1996).

³S. I. Kiselev, J. C. Sankey, I. N. Krivorotov, N. C. Emley, R. J. Schoelkopf, R. A. Buhrman, and D. C. Ralph, *Nature (London)* **425**, 380 (2003).

⁴S. Kaka, M. R. Pufall, W. H. Rippard, T. J. Silva, S. E. Russek, and J. A. Katine, *Nature (London)* **437**, 389 (2005).

⁵L. Thomas, M. Hayashi, X. Jiang, R. Moriya, C. Rettner, and S. S. P. Parkin, *Nature (London)* **443**, 197 (2006).

⁶S. S. P. Parkin, US Patent 309,6,834,005 (2004).

⁷D. A. Allwood, G. Xiong, C. C. Faulkner, D. Atkinson, D. Petit, and R. P. Cowburn, *Science* **309**, 1688 (2005).

⁸M. Hayashi, L. Thomas, Ya. B. Bazaliy, C. Rettner, R. Moriya, X. Jiang, and S. S. P. Parkin, *Phys. Rev. Lett.* **96**, 197207 (2006).

⁹F. Junginger, M. Kläui, D. Backes, U. Rüdiger, T. Kasama, R. E. Dunin-Borkowski, L. J. Heyderman, C. A. F. Vaze, and J. A. C. Bland, *Appl. Phys. Lett.* **90**, 132506 (2007).

¹⁰A. Yamaguchi, S. Nasu, H. Tanigawa, T. Ono, K. Miyake, K. Mibu, and T. Shinjo, *Appl. Phys. Lett.* **86**, 012511 (2005).

¹¹C.-Y. You, I. M. Sung, and B.-K. Joe, *Appl. Phys. Lett.* **89**, 222513 (2006).

¹²C.-Y. You and S.-S. Ha, *Appl. Phys. Lett.* **91**, 022507 (2007).

¹³The waveguide structure with 50 Ω impedance is employed for better transmission. The waveguide was made of 100-nm-thick copper strip line surrounded by the ground plane deposited on Si wafer. The ratio of the line width and the gap distance is kept constant to be 0.7 for impedance matching. The coaxial cables are directly connected to the electrodes of the strip line and the ground.

¹⁴The solid line in Fig. 2(a) is used as the input voltage pulse profile.